Quest Journals
Journal of Research in Applied Mathematics
Volume 11 ~ Issue 12 (December 2025) pp: 145-155
ISSN (Online): 2394-0743 ISSN (Print): 2394-0735
www.questjournals.org

Research Paper

A Modified Homotopy Perturbation Method for Efficient Analysis of Nonlinear Rotating Pendulum Dynamics

Adel Ahmed Hassan Kubba[(1)], OMER SALEH IBRAHIM MAHMOUD [(2)]
(1)Associate Professor - Nile Valley University - Faculty of Education
(2)Student

Abstract:
This paper presents a development and enhancement of the Modified Homotopy Perturbation Method (MHPM) for solving strongly nonlinear oscillatory problems, with application to the rotating pendulum model. The method allows for obtaining highly accurate approximate solutions for frequency and time response without the need to expand trigonometric functions like sine into Taylor series, thereby preserving accuracy even at large deflection angles. The results are compared with other established methods such as the Homotopy Analysis Method (HAM), Gamma Function Method (GFM), and Harmonic Balance Method (HBM). MHPM demonstrates clear superiority in terms of accuracy and relative error, especially at large amplitudes and high rotational speeds. The study provides a detailed analysis of the influence of rotational speed (Λ) and amplitude (A) on the system's dynamics and confirms the method's efficiency in modeling complex nonlinear systems.

Keywords:
Modified Homotopy Perturbation Method, rotating pendulum, nonlinear vibrations, approximate frequency, comparative analysis, nonlinear dynamical systems.

*Received 15 Dec., 2025; **R**evised 28 Dec., 2025; **A**ccepted 30 Dec., 2025 © The author(s) 2025.*
P**ublished with open access at **www.questjournas.org

I. Introduction

Many engineering problems can be modeled by nonlinear ordinary or partial differential equations, but obtaining exact solutions is often highly complex or even impossible, with only a few exceptions. This complexity arises from the intrinsic nature of nonlinearity, where interactions between variables are not directly proportional, leading to behaviors such as bifurcations, chaos, and other intricate dynamics. As a result, asymptotic solutions, which approximate solutions under specific limiting conditions, have gained significant attention among scientists and engineers tackling various nonlinear equations.

For weakly nonlinear problems, classical methods like the averaging method and the small parameter method have been commonly employed. These techniques simplify the original problem into a form that can be more easily analyzed, often by isolating dominant terms and treating others as perturbations. In addition to these foundational approaches, more advanced methods such as the multiple scales (MS) method and the Lindstedt–Poincare (LP) method have been developed. These methods offer valuable advantages in solving vibratory systems by addressing resonance and periodic solutions in nonlinear dynamics. However, their accuracy critically depends on the proper selection of a small parameter, and an incorrect choice may lead to erroneous or physically unrealistic solutions.[1]

II. Modified homotopy perturbation method

For describing the method at first, we take into account an oscillator with strong nonlinearity as [2]

(1)

$$\ddot{u} + \omega_0^2 u + f(u, \dot{u}, \ddot{u}) = 0,$$

where the dots over the variable u represent derivative with respect to time, t, unperturbed frequency of the oscillator is ω_0 and the nonlinear function is represented by f $(u, \dot{u}, \ddot{u})$. The initial conditions of the oscillator are given as

$$u(0) = A, \dot{u}(0) = 0. \tag{2}$$

If we chose $\tau = \omega t$, equation (1) is transformed to

(3)

$$\omega^2 u'' + \omega_0^2 u + f(u, \omega u', \omega^2 u'') = 0,$$

where primes on u represent derivative with respect to τ and the initial conditions are transformed as u (0) = A, u′(0)= 0. We consider the homotopy for the equation (3) as

$$\omega^2 u' + \omega^2 u + p\,(-\omega^2 u + \omega^2{}_0 u + f(u, \omega u', \omega^2 u'')) = 0: \tag{4}$$

According to the present MHPM, solution of the equation (4) is considered as

$$u = u_0 + pu_1 + p^2 u_2 + p^3 u_3 + \ldots, \tag{5}$$

while the frequency response is considered as

$$\omega^2 = \omega^2{}_0\,(1 + p\omega_1 + p^2\omega_2 + p^3\omega_3 + \ldots). \tag{6}$$

We now use the values of u and ω^2 from equations (5) and (6) into equation (4) and expand the resulting equation in a power series of p and then equate the coefficient of various powers of p from both sides to get a set of linear differential equations. These equations are solved in sequence to determine the solution and frequency response.[2]

We can see from equation (4), as p→1, it reduces to equation (1), whereas equations (5) and (6) are written as

$$u = u_0 + u_1 + u_2 + u_3 + \ldots, \tag{7}$$

and

$$\omega^2 = \omega^2{}_0(1 + \omega_1 + \omega_2 + \omega_3 + \ldots). \tag{8}$$

The MHPM solution and frequency response of equation (1) is thus represented by equations (7) and (8).

III. Examples

The rotating pendulum (3.1)[3] The subsequent implementation, as illustrated in Figure 3.1, utilizes nonlinear differential equations (NLDEs) to thoroughly simulate the dynamic behavior of a simple pendulum attached to a rotating solid framework. By integrating NLDEs, the model offers a more precise and realistic depiction of the pendulum's response to rotational influences. The system's governing equation of motion is

$$\ddot{u} + (1 - A\cos u)\sin u = 0, \tag{9}$$

where $\Lambda = \frac{\Omega^2 r}{g}$ and the initial conditions are specified as u(0) =A, $\dot{u}$ (0)= 0.

If ω represents the frequency of the oscillator, equation (9) can be expressed as

$$\omega^2 u'' + (1 - \Lambda \cos u) \sin u = 0, \tag{10}$$

where $\tau = \omega t$, $u' = \frac{du}{dt}$ and the initial conditions are converted to $u(0) = A$,

$u'(0) = 0$: According to the present method the homotopy for equation (10) is considered as

$$\omega^2 u'' + \omega^2 u (-\omega^2 u + \sin u - \Lambda \cos x \sin x) = 0, \tag{11}$$

Substituting the values of u and ω^2 from equations (5) and (6) into equation (11) and equating the terms from both sides with the same powers of p, we can derive a series of linear differential equations, of which we present onlv the first three as

$$\omega_0^2 u_0'' + \omega_0^2 u_0 = 0;\ u_0(0) = A, u_0'(0) = 0 \tag{12}$$

$$\omega_0^2 u_1'' + \omega_0^2 u_1 = u_0\omega_0^2 - \sin u_0 + \Lambda \cos u_0 \sin u_0 - u_0\omega_0^2\omega_1 - u_0''\omega_0^2\omega_1;\ u_1(0) = 0, u_1'(0) = 0 \tag{13}$$

$$\begin{aligned}\omega_0^2 u_2'' + \omega_0^2 u_2 = {} & u_1\omega_0^2 - u_1 \cos u_0 + \Lambda u_1 \cos^2 u_0 - \Lambda u_1 \sin^2 u_0 + u_0\omega_0^2\omega_1 - u_1\omega_0^2\omega_1 \\ & - u_1''\omega_0^2\omega_1 - u_0\omega_0^2\omega_2 - u_0''\omega_0^2\omega_2;\ u_1(0) = 0, u_1'(0) = 0\end{aligned} \tag{14}$$

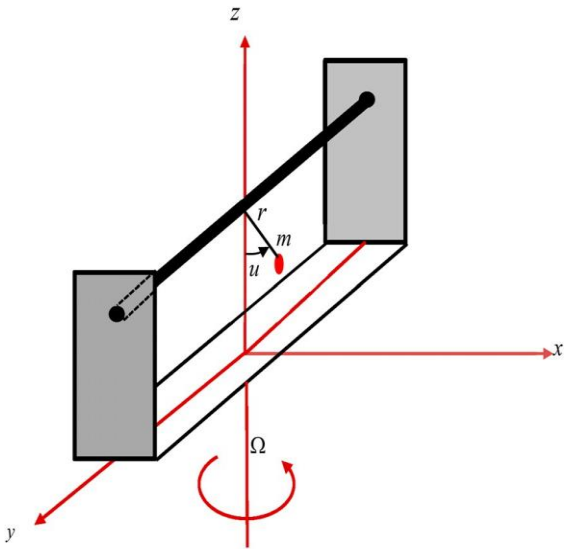

Figure 3.1. Schematic of a rotating pendulum.

The solution of equation (12) is

$$u_0 = A \cos \tau \tag{15}$$

By substituting the value of u_0 into equation (13) and simplifying, we obtain

$$\omega_0^2 u_1'' + \omega_0^2 u_1 = \omega_0^2 A \cos\tau - \sin(A\cos\tau) + \Lambda \sin(A\cos\tau)\cos(A\cos\tau) = \omega_0^2 A\cos\tau - \sin(A\cos\tau) + \frac{\Lambda}{2}\sin(2A\cos\tau) \tag{16}$$

Fourier series expansions for sin(A cos τ) and sin(2 A cos τ) are considered as

$$\sin(A\cos\tau) = \sum_{n=0}^{\infty} l_{2n+1} \cos[(2n+1)\tau] = l_1 \cos\tau + l_3 \cos 3\tau + \ldots, \tag{17}$$

where

and $$l_{2n+1} = \frac{4}{\pi}\int_0^{\pi/2} sin(A\,cos\,\tau)cos[(2n+1)\tau]d\tau = 2(-1)^n J_{2n+1}(A), \tag{18}$$

$$sin(2A\,cos\,\tau) = \sum_{n=0}^{\infty} e_{2n+1}\,cos[(2n+1)\tau] = e_1\,cos\,\tau + e_3\,cos\,3\tau + \ldots, \tag{19}$$

where

$$e_{2n+1} = \frac{4}{\pi}\int_0^{\pi/2} sin(2A\,cos\,\tau)cos[(2n+1)\tau]d\tau = 2(-1)^n J_{2n+1}(2A). \tag{20}$$

We consider $I_{2n+1}(A)$ as the Bessel function of the first kind of (2n+1)-order. The first term for both these series is obtained as $l_1 = 2J_1(A)$ and $e_1 = 2J_1(2A)$. Where $J_1(A)$ is the first-order Bessel function of the first kind. Substitution of these results into equation (16) gives

$$\omega_0^2 u_1'' + \omega_0^2 u_1 = \omega_0^2 A\,cos\,\tau - 2J_1(A)cos\,\tau + AJ_1(2A)cos\,\tau - \sum_{n=1}^{\infty} l_{2n+1}\,cos[(2n+1)\tau] + \frac{k}{2}\sum_{n=1}^{\infty} e_{2n+1}\,cos[(2n+1)\tau]. \tag{21}$$

Avoiding secular term, we get

$$\omega_0^2 = \frac{2J_1(A) - AJ_1(2A)}{A}. \tag{22}$$

Thus, the zeroth-order approximate frequency is

$$\omega_0 = \sqrt{\frac{2J_1(A) - AJ_1(2A)}{A}}. \tag{23}$$

Which is same as the first-order approximate frequency determined by Moatimid et al. Remaining part of equation (21) is written as follows:

$$\omega_0^2 u_1'' + \omega_0^2 u_1 = \frac{A}{2}\sum_{n=1}^{\infty} e_{2n+1}\,cos[(2n+1)\tau] - \sum_{n=1}^{\infty} l_{2n+1}\,cos[(2n+1)\tau], \tag{24}$$

with initial conditions $u_1(0) = 0$, $u^0{}_1(0) = 0$. The solution to equation (24) is chosen as follows:

$$u_1 = \sum_{n=0}^{\infty} b_{2n+1}\,cos[(2n+1)\tau]. \tag{25}$$

Substituting equations (4.2.25) into (4.2.24) gives

$$-\omega_0^2\sum_{n=1}^{\infty} 4n(n+1)b_{2n+1}\,cos[(2n+1)\tau] = \frac{A}{2}\sum_{n=1}^{\infty} e_{2n+1}\,cos[(2n+1)\tau] - \sum_{n=1}^{\infty} l_{2n+1}\,cos[(2n+1)\tau], \tag{26}$$

and then we can write the following expression for the coefficients b_{2n+1}:

$$b_{2n+1} = \frac{l_{2n+1}}{4n(n+1)\omega_0^2} - \frac{Ae_{2n+1}}{8n(n+1)\omega_0^2} = \frac{2(-1)^2 J_{2n+1}(A)}{4n(n+1)\omega_0^2} - \frac{A(-1)^2 J_{2n+1}(2A)}{4n(n+1)\omega_0^2}, \quad (27)$$

for $n \geq 1$. Considering that $u_1(0) = 0$, equation (25) gives

$$b_1 = -\sum_{n=1}^{\infty} b_{2n+1}. \quad (28)$$

From equation (14), it is obvious that the value of u_1 is required to determine the higher-order approximate solution u_2. But u_1 has infinite number of terms, which will create difficulties to obtain the higher-order solution u_2. However, we can truncate the series expansion of u_1 presented in equation (25) and express an approximate equation $u_1^{(N)}$ in the form

$$b_1^{(N)} = -\sum_{n=1}^{N} b_{2n+1}, \quad (29)$$

and

$$u_1^{(N)} = \sum_{n=0}^{N} b_{2n+1} \cos[(2n+1)\tau], \quad (30)$$

which contains only a finite number of harmonics. By comparing equations (25) and (29), we find that

$$\lim_{N \to \infty} u_1^{(N)} = u_1, \quad (31)$$

$$\lim_{N \to \infty} b_1^{(N)} = b_1. \quad (32)$$

For simplicity, we can consider N = 2 in equation (4.2.29) and we obtain

$$u_1^{(2)} = b_1^{(2)} \cos\tau + b_3 \cos 3\tau = b_3(\cos 3\tau - \cos\tau) + b_5(\cos 5\tau - \cos\tau), \quad (33)$$

$$b_3 = \frac{l_3}{8\omega_0^2} - \frac{Ae_3}{16\omega_0^2}, \quad (34)$$

$$b_5 = \frac{l_5}{24\omega_0^2} - \frac{Ae_5}{48\omega_0^2},$$

where l_3, l_5, e_3 and e_5 are given. Thus, the first-order approximate solution is

$$u_1^{(2)} = b_3(\cos 3\tau - \cos\tau) + b_5(\cos 5\tau - \cos\tau). \quad (35)$$

The first approximate frequency ω_1 can be derived by applying the no secular term condition on equation (14). Now substituting the value of u_0 and $u_1^{(2)}$, equation (14) becomes

$$\omega_0^2 u_2'' + \omega_0^2 u_2 = \omega_0^2(b_3(\cos 3\tau - \cos\tau) + b_5(\cos 5\tau - \cos\tau))$$
$$-(b_3(\cos 3\tau - \cos\tau) + b_5(\cos 5\tau - \cos\tau))\cos(A\cos\tau) + A(b_3(\cos 3\tau - \cos\tau) + b_5(\cos 5\tau$$
$$-\cos\tau))\cos(2A\cos\tau) + \omega_0^2\omega_1 A\cos\tau - \omega_0^2\omega_1(b_3(\cos 3\tau - \cos\tau) + b_5(\cos 5\tau - \cos\tau))$$
$$+\omega_0^2\omega_1(b_3(9\cos 3\tau - \cos\tau) + b_5(25\cos 5\tau - \cos\tau)).$$

(36)

It is possible to do the following Fourier series expansion

$$(\cos 3\tau - \cos\tau)\cos(A\cos\tau) = \sum_{n=0}^{\infty} m_{2n+1}\cos[(2n+1)\tau] = m_1\cos\tau + m_3\cos 3\tau + \ldots, \quad (37)$$

$$(\cos 5\tau - \cos\tau)\cos(A\cos\tau) = \sum_{n=0}^{\infty} n_{2n+1}\cos[(2n+1)\tau] = n_1\cos\tau + n_3\cos 3\tau + \ldots, \quad (38)$$

$$(\cos 3\tau - \cos\tau)\cos(2A\cos\tau) = \sum_{n=0}^{\infty} f_{2n+1}\cos[(2n+1)\tau] = f_1\cos\tau + f_3\cos 3\tau + \ldots, \quad (39)$$

and

$$](\cos 5\tau - \cos\tau)\cos(2A\cos\tau) = \sum_{n=0}^{\infty} g_{2n+1}\cos[(2n+1)\tau] = g_1\cos\tau + g_3\cos 3\tau + \ldots, \quad (40)$$

$$\omega_1 = \frac{b_3 m_1 + b_5 n_1 + \omega_0^2 b_3 + \omega_0^2 b_5 - A b_3 f_1 - A b_5 g_1}{A\omega_0^2}, \quad (41)$$

where m_1, n_1, f_1 and g_1 are given.

Thus, the first-order approximate frequency is

$$\omega = \sqrt{\omega_0^2(1+\omega_1)}, \quad (42)$$

where ω_0,ω_1 are given by equation (23) and (41), respectively, and the corresponding first-order approximate solution is

$$u = (A - b_3 - b_5)\cos\omega t + b_3\cos 3\omega t + b_5\cos 3\omega t, \quad (43)$$

where b_3, b_5 are given by equation (34).

IV. Results and discussion

We provide a comprehensive analysis of the accuracy and efficiency of the modified homotopy perturbation method (MHPM) across a range of parameters, highlighting its superior performance in frequency and period approximations. Notably, the first-order approximation of frequencies using MHPM delivers exceptionally accurate results for both examples. A critical advancement in this work is the decision to retain the sine function in its entirety rather than employing a Taylor series expansion, as is common in many traditional methods for solving the rotating pendulum equation. While Taylor series expansions are effective for small deflection angles, they introduce significant errors as the pendulum's deflection approaches higher degrees. In contrast, retaining the full sine function allows MHPM to maintain high accuracy, even for large deflection angles.[4]

Detailed comparisons with established methods such as the homotopy analysis method (HAM), gamma function method (GFM), and the coupled method underscore the precision of MHPM. These comparisons, presented in Tables 4.1– 4.3, validate the efficacy of the method across various amplitude values. For instance,

in the case of a rotating frame pendulum with $\Lambda = 0.1$ and $A = 170°$, the maximum relative error for the first approximate frequency using MHPM is just 2.35%. In comparison, the Coupled Method and HAM report significantly higher maximum relative errors of 16.97% under the same conditions. Additionally, the GFM demonstrates an even larger relative error of approximately 74.07% for the first approximate frequency at $\Lambda = 0.1$ and $A = 160°$.

Figures 4.2 and 4.2 visually corroborate these findings, illustrating the high accuracy of MHPM for larger amplitudes. The solutions obtained using MHPM closely align with exact solutions, demonstrating the method's robustness and reliability.

Figure 4.2 explores the dual effects of rotational speed (Λ) and amplitude (A) on the rotational pendulum's time period when length r is constant, revealing two distinct trends: At low rotational speeds $\Lambda = 0.1$, the time period increases with amplitude A, as the rotational speed has minimal influence on pendulum oscillations. Under these conditions, the system behaves similarly to a simple pendulum. At higher rotational speeds $\Lambda \geq 0.5$, the rotational speed significantly affects the oscillatory dynamics, leading to a decrease in the time period as A increases. This behavior highlights the pronounced role of rotational speed in shaping the pendulum's dynamics.[5]

To further evaluate the performance of MHPM, the approximate period are compared to the exact period for the simple pendulum equation, given by

(44)

$$T_{ex} = T_0\left(1 + \frac{A^2}{16} + \frac{11A^4}{3072} + \frac{173A^6}{737280} + \frac{22931A^8}{1321205760} + \cdots\cdots\right),$$

where $T_0 = 2\pi\sqrt{1/k}$.

The first approximate period using MHPM is

(45)

$$T_{MHPM1} = T_0\left(1 + \frac{A^2}{16} + \frac{11A^4}{3072} + \frac{175A^6}{737280} + \frac{23618A^8}{1321205760} + \cdots\cdots\right),$$

with a limiting value

(46)

$$\lim_{A \to 180} \frac{T_{MHPM1}}{T_{ex}} \cong 1.029952.$$

By contrast, the second approximate period from the harmonic balance method (HBM) is

(47)

$$T_{HBM2} = T_0\left(1 + \frac{A^2}{16} + \frac{10A^4}{3072} + \frac{90A^6}{737280} + \cdots\cdots\right),$$

with a limiting value of

(48)

$$\lim_{A \to 180} \frac{T_{HBM2}}{T_{ex}} \cong 0.520414.$$

Similarly, the second approximate period from the standard homotopy perturbation method (HPM) is

(49)

$$T_{HPM2} = T_0\left(1 + \frac{A^2}{16} + \frac{11A^4}{3072} + \frac{173A^6}{737280} + \frac{23898A^8}{1321205760} + \cdots\cdots\right)$$

with a limiting value of

$$\lim_{A \to 180} \frac{T_{HPM2}}{T_{ex}} \cong 1.042150. \tag{50}$$

These comparisons highlight the superior performance of MHPM, which achieves lower relative errors even in its first approximation compared to the higher-order approximations of HBM and HPM.

The results unequivocally demonstrate that MHPM provides a highly accurate and efficient framework for predicting the dynamics of pendulums, particularly under conditions of large deflection angles and for both high and low rotational speeds. By retaining the full sine function and employing a novel approach to approximations, MHPM overcomes the limitations of traditional methods, offering significant advancements in modeling complex nonlinear oscillatory systems.[6]

Table 4.1. Comparison among frequencies obtained various methods for $\Lambda = 0.1$.

A	ω_e	ω_{HAM1} Er(%)	$\omega_{Coupled1}$ Er(%)	ω_{HMPM1} Er(%)	ω_{GTM1} Er(%)
10°	0.947477	0.947476781	0.947476781	0.947477	0.947475
		0.0000	0.0000	0.0000	00.0000
20°	0.943828	0.943830354	0.943830354	0.943828	0.943794
		0.0002	0.0002	0.0000	0.0004
30°	0.937654	0.937665034	0.937665034	0.937654	0.937477
		0.0012	0.0012	0.0000	0.0189
40°	0.928817	0.928854277	0.928854277	0.928817	0.928254
		0.0040	0.0040	0.0000	0.0606
50°	0.917139	0.917234548	0.917234548	0.917139	0.915752
		0.0104	0.0104	0.0000	0.1513
60°	0.902406	0.902619454	0.902619454	0.902406	0.899491
		0.0237	0.0237	0.0000	0.3230
70°	0.884376	0.884805719	0.884805719	0.884376	0.878884
		0.0486	0.0486	0.0000	0.6210
80°	0.862791	0.863595013	0.863595013	0.862792	0.853214
		0.0932	0.0932	0.0001	1.1100
90°	0.837376	0.838798882	0.838798882	0.837379	0.8216
		0.1699	0.1699	0.0003	1.8840
100°	0.80784	0.810251805	0.810251805	0.807848	0.782916
		0.2986	00.2986	00.0010	3.0852
110°	0.773857	0.777818648	0.777818648	0.773877	0.735652
		0.5119	0.5119	0.0026	4.9370
120°	0.73504	0.741393859	0.741393859	0.735092	0.677616
		0.8644	0.8644	0.0071	7.8124
130°	0.690863	0.700900159	0.700900159	0.690994	0.605291
		1.4529	1.4529	0.0190	12.3862
140°	0.640508	0.656274005	0.656274005	0.640844	0.512149
		2.4615	2.4615	0.0525	20.0402
150°	0.5825	0.607441391	0.607441391	0.583403	0.382525
		4.2818	4.2818	0.1550	34.3305
160°	0.513636	0.554273622	0.554273622	0.51632	0.133175
		7.9118	7.9118	0.5226	74.0720
170°	0.424456	0.49650052	0.49650052	0.434412	------
		16.9735	16.9735	1.023458	------

Where Er(%) represents absolute percentage error.

Table 4.2. Comparison among frequencies obtained various methods for $\Lambda = 0.5$.

A	ω_e	ω_{HAM1} $Er(\%)$	$\omega_{Coupled1}$ $Er(\%)$	ω_{HAPM1} $Er(\%)$	ω_{GTM1} $Er(\%)$
10°	0.70977	0.709770265	0.709770265	0.70977	0.709769
		0.0001	0.0001	0.0000	0.0000
20°	0.717411	0.717422729	0.717422729	0.717411	0.717396
		0.0016	0.0016	0.0000	0.0021
30°	0.729059	0.729107729	0.729107729	0.729059	0.728973
		0.0067	0.0067	0.0000	0.0118
40°	0.743283	0.743399142	0.743399142	0.743283	0.742984
		0.0156	0.0156	0.0000	0.0403
50°	0.758405	0.758602593	0.758602593	0.758405	0.757608
		0.0261	0.0261	0.0000	0.1051
60°	0.772676	0.77293577	0.77293577	0.772678	0.770911
		0.0336	0.0336	0.0002	0.2284
70°	0.784415	0.78468068	0.78468068	0.784417	0.780987
		0.0339	0.0339	0.0003	0.4370
80°	0.792082	0.792285208	0.792285208	0.792085	0.786044
		0.0257	0.0257	0.0004	0.7623
90°	0.79432	0.794422737	0.794422737	0.794321	0.784444
		0.0129	0.0129	0.0001	1.2434
100°	0.789963	0.790016374	0.790016374	0.789959	0.774691
		0.0067	0.0067	0.999994	1.9333
110°	0.778014	0.778250675	0.778250675	0.778	0.755375
		0.0304	0.0304	0.999982	2.9099
120°	0.757597	0.758555771	0.758555771	0.757579	0.706021
		0.1265	0.1265	0.999976	6.8079
130°	0.727867	0.730586629	0.730586629	0.727877	0.681997
		0.3737	0.3737	0.0014	6.3019
140°	0.687817	0.694187166	0.694187166	0.687968	0.623785
		0.9262	0.9262	0.0220	9.3094
150°	0.635859	0.649335149	0.649335149	0.636513	0.546182
		2.1193	2.1193	0.1028	14.1033
160°	0.568623	0.596063604	0.596063604	0.571044	0.440009
		4.8258	4.8258	0.4257	22.6185
170°	0.475894	0.534319635	0.534319635	0.485938	0.275313
		12.2770	12.2770	2.1106	42.1483

Where Er(%) represents absolute percentage error.

Table 4.3. Comparison among frequencies obtained various methods for $\Lambda = 0.9$.

A	ω_e	ω_{HAM1} Er(%)	$\omega_{Coupled1}$ Er(%)	ω_{HMPM1} Er(%)	ω_{GFM1} Er(%)
10°	0.331359	0.331414417	0.331414417	0.331359	0.331412
		0.0166	0.0166	0.0000	0.0160
20°	0.371673	0.372256865	0.372256865	0.371674	0.372245
		0.1572	0.1572	0.0004	0.1540
30°	0.427181	0.428928525	0.428928525	0.427195	0.428885
		0.4092	0.4092	0.0033	0.3990
40°	0.489305	0.492459206	0.492459206	0.48935	0.492333
		0.6447	0.6447	0.0093	0.6190
50°	0.552065	0.556450032	0.556450032	0.552157	0.556183
		0.7943	0.7943	0.0166	0.7460
60°	0.611366	0.61655304	0.61655304	0.611509	0.616055
		0.8484	0.8484	0.0234	0.7670
70°	0.664303	0.669750116	0.669750116	0.664491	0.668914
		0.8199	0.8199	0.0283	0.6940
80°	0.708738	0.713887975	0.713887975	0.708955	0.712565
		0.7266	0.7266	0.0306	0.5400
90°	0.743058	0.747415522	0.747415522	0.743277	0.745436
		0.5864	0.5864	0.0295	0.3200
100°	0.766035	0.769248686	0.769248686	0.766223	0.76638
		0.4195	0.4195	0.0245	0.0450
110°	0.776727	0.778682523	0.778682523	0.776841	0.774595
		0.2518	0.2518	0.0147	0.2744
120°	0.774385	0.775337331	0.775337331	0.774383	0.769562
		0.1230	0.1230	0.999998	0.3228
130°	0.758335	0.759113271	0.759113271	0.758193	0.750908
		0.1026	0.1026	0.999813	0.9794
140°	0.727766	0.730134472	0.730134472	0.727526	0.718275
		0.3254	0.3254	0.999670	1.3042
150°	0.681266	0.688685168	0.688685168	0.681204	0.671047
		1.0890	1.0890	0.999908	1.5000
160°	0.61552	0.635109687	0.635109687	0.6168	0.607849
		3.1826	3.1826	0.2079	1.2463
170°	0.519821	0.569633982	0.569633982	0.528323	0.525362
		9.5827	9.5827	01.6355	1.0660

Where Er(%) represents absolute percentage error.

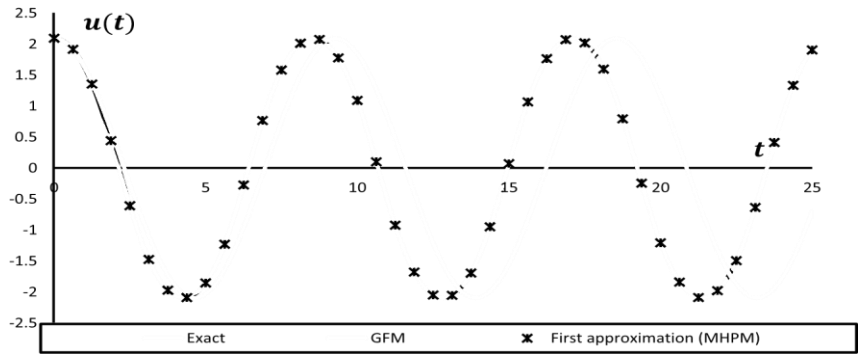

Figure 4.2. Comparison among the solutions obtained by the modified homotopy perturbation method (MHPM), gamma function method (GFM) with exact solution for $\Lambda = 0.1$, $A = 120°$.

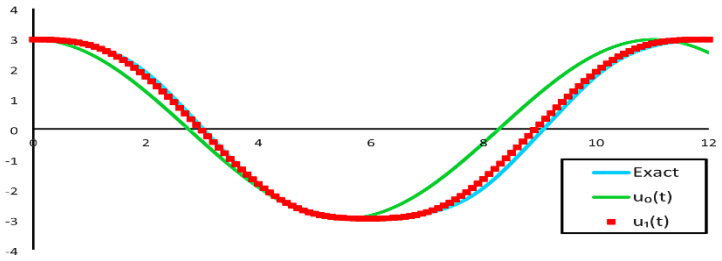

Figure 4.3. Comparison among the zeroth and first-order solutions obtained by the modified homotopy perturbation method (MHPM) with exact solution for $\Lambda = 0.9$, $A = 170°$.

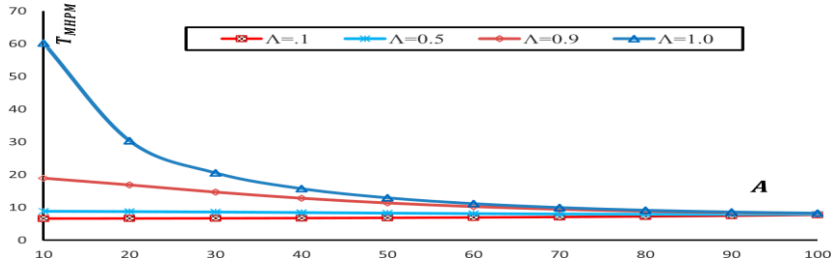

Figure 4.4. Variation of first approximate period obtained by the modified homotopy perturbation method(MHPM) for various values of the parameter Λ.

V. Conclusion

This paper presents an enhanced application of the Modified Homotopy Perturbation Method (MHPM) to study the nonlinear motion of a rotating pendulum. The method successfully provides high-accuracy estimates for frequency and time period without linearizing the sine function, making it effective even at large amplitudes. Results demonstrate the superiority of MHPM over traditional methods such as HAM, GFM, and HBM in terms of accuracy and convergence speed. The study also highlights the influence of rotational speed and amplitude on the system's behavior, underscoring the value of MHPM in analyzing complex nonlinear dynamical systems.

References

[1]. He, J. H. (1999). Homotopy perturbation technique. Computer Methods in Applied Mechanics and Engineering, 178(3-4), 257–262.
[2]. He, J. H. (2003). A simple perturbation approach to Blasius equation. Applied Mathematics and Computation, 140(2-3), 217–222.
[3]. He, J. H. (2006). Some asymptotic methods for strongly nonlinear equations. International Journal of Modern Physics B, 20(10), 1141–1199.
[4]. Liao, S. J. (2003). Beyond perturbation: introduction to the homotopy analysis method. Chapman and Hall/CRC.
[5]. Moatimid, G. M., Elagamy, K., & Hassan, M. H. (2020). Nonlinear oscillators: a coupled method of the homotopy perturbation method with the energy balance method. Journal of Applied and Computational Mechanics, 6(3), 447–460.
[6]. Nayfeh, A. H., & Mook, D. T. (2008). Nonlinear oscillations. John Wiley & Sons.
[7]. Öziş, T., & Yıldırım, A. (2007). A comparative study of He's homotopy perturbation method for determining frequency-amplitude relation of a nonlinear oscillator with discontinuities. International Journal of Nonlinear Sciences and Numerical Simulation, 8(2), 243–248.
[8]. Ramos, J. I. (2007). A review of some approximate methods for solving nonlinear oscillators. Scientific Research and Essays, 2(2), 031–057.
[9]. Shou, D. H., & He, J. H. (2007). Application of parameter-expanding method to strongly nonlinear oscillators. International Journal of Nonlinear Sciences and Numerical Simulation, 8(1), 121–124.
[10]. Wu, B. S., Sun, W. P., & Lim, C. W. (2006). An analytical approximate technique for a class of strongly nonlinear oscillators. International Journal of Nonlinear Mechanics, 41(6-7), 766–774.